Inversion of the Current-Distance Relationship by Transient Depolarization

Warren M. Grill,* *Member, IEEE*, and J. Thomas Mortimer

Abstract—**The objective of this research was to develop a technique to excite selectively nerve fibers distant from an electrode without exciting nerve fibers close to the electrode. The shape of the stimulus current waveform was designed based on the nonlinear conductance properties of neuronal sodium channels. Models of mammalian peripheral myelinated axons and experimental measurements on cat sciatic nerve were used to determine the effects of subthreshold polarization on neural excitability and recruitment. Subthreshold membrane depolarization generated a transient decrease in neural excitability and thus an increase in the threshold for stimulation by a subsequent stimulus pulse. The decrease in excitability increased as the duration and amplitude of the subthreshold depolarization were increased, and the increase in threshold was greater for fibers close to the electrode. When a depolarizing stimulus pulse was applied immediately after the subthreshold depolarization, nerve fibers far from the electrode could be stimulated without stimulating fibers close to the electrode. Subthreshold depolarizing prepulses inverted the current-distance relationship and allowed selective stimulation of nerve fibers far from the electrode.**

Index Terms—**Current-distance relationship, electrical stimulation, electrode, nerve stimulation, sodium inactivation, stimulus waveform.**

I. Introduction

SELECTIVE stimulation of neurons within the central and peripheral nervous systems is a powerful tool to study neural function and a requirement for multichannel neural prosthetic devices [17]. For example, stimulation of discrete populations of cochlear nerve fibers allows exploitation of the tonotopic map of the cochlea in auditory prostheses [5], [27], and selective stimulation of peripheral nerve fascicles allows independent control of the contraction strength generated in individual skeletal muscles innervated by a common nerve trunk [14], [35]. Electrode designs presently under development for selective stimulation of peripheral nerve trunk fascicles include multiple contact nerve cuff electrodes [14], [35], intrafascicular wire electrodes [38], intrafascicular silicon electrodes [24], and wire electrodes sutured to the epineurium [30]. These electrodes will provide the technology for more functional motor prostheses that can be applied to larger numbers of individuals with neurological impairments.

Nerve-based electrodes share the common goal of stimulating a discrete region of a peripheral nerve trunk. Selectivity has been accomplished by placing multiple, spatially distributed electrode contacts in or on different regions of a nerve trunk. Using conventional stimuli (e.g., 100-μs rectangular current pulses), nerve fibers lying closer to an electrode are recruited at lower current amplitudes than required to excite more distant fibers. The threshold current for excitation of myelinated nerve fibers is proportional to the square of the distance from the electrode to the nerve fiber [2], [7], [22], [37]. Thus, proximity of the electrode to the nerve fibers targeted for activation has been one means to achieve selectivity.

A second method to achieve selectivity is the use of field shaping. Subthreshold field steering currents have been used to improve selectivity of peripheral nerve stimulation with nerve cuff electrodes [14], [29], [35]. These currents do not generate excitation, but alter the region of activation generated by the stimulus pulse. Similarly, field shaping using current application to multiple electrodes has been used to improve selectivity in cochlear prostheses [23], [31].

The choice of stimulus waveform can also affect neuronal selectivity. Short duration current pulses increase the threshold difference between nerve fibers of different diameters and thus produce more easily graded muscle contractions [10]. Short stimulus pulsewidths also increase the slope of the current-distance-relationship, thus increasing the threshold difference between nerve fibers at different distances from the electrode [13]. Modeling and experimental studies have demonstrated that a secondary stimulus phase, used for charge recovery, can abolish action potentials in nerve fibers excited just above threshold. The abolition of action potentials depended on the shape, amplitude, and duration of the secondary phase and was eliminated by an interphase delay [32]. Thus, for a particular electrode geometry, the choice of stimulus parameters affects the population of nerve fibers that will be stimulated.

The objective of this research was to develop stimulation waveforms to excite nerve fibers distant from an electrode without exciting nerve fibers close to the electrode. Such a technique would allow selective stimulation of nerve fibers lying deep in a nerve trunk without the risk of neural damage associated with penetrating electrodes [25]. Stimulus waveforms were designed to invert of the slope of the current-distance relationship by exploiting the nonlinear conductance properties of the neural membrane. Inversion of the current-distance relationship allowed stimulation of fibers lying more

Manuscript received February 10, 1995; revised August 2, 1996. This work was supported in part by a Grant from the Paralyzed Veterans of America Spinal Cord Research Foundation and by the NIH NINDS Neural Prosthesis Program under Grant N01-NS-3-2300. *Asterisk indicates corresponding author.*

*W. M. Grill is with the Applied Neural Control Laboratory, Department of Biomedical Engineering, Case Western Reserve University, C.B. Bolton Bldg. 3480, Cleveland, OH 44106-4912 USA (e-mail: wmg@po.cwru.edu).

J. T. Mortimer is with the Applied Neural Control Laboratory, Department of Biomedical Engineering, Case Western Reserve University, Cleveland, OH 44106-4912 USA.

Publisher Item Identifier S 0018-9294(97)00603-4.

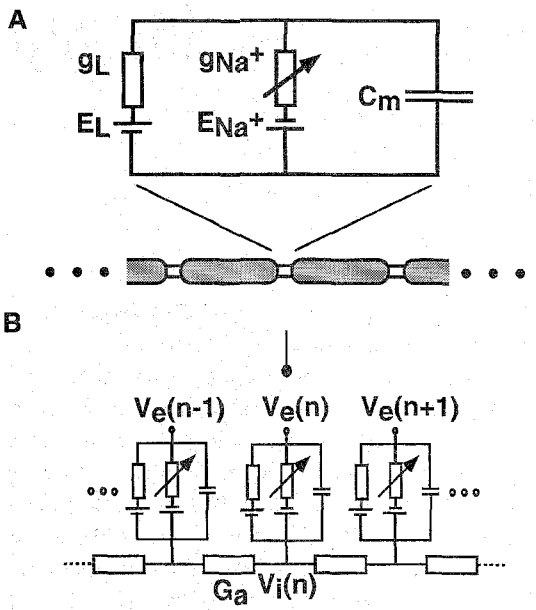

Fig. 1. Models of mammalian peripheral nerve fibers: (A) model of a single node of Ranvier including the nonlinear sodium conductance $g_{\mathrm{Na}+}$, the sodium Nernst battery $E_{\mathrm{Na}+}$, the linear leakage conductance g_L, the leak Nernst battery E_L, and the membrane capacitance C_m and (B) cable model of a nerve fiber was positioned in the extracellular potentials $V_e(n)$, generated by a point source electrode. Each node of Ranvier was modeled using the circuit of (A) and the nodes were connected intracellularly by the axial conductance G_a.

distant from an electrode at lower currents than required to stimulate fibers lying close to the electrode. Preliminary results of this study have been published in abstract form [15] and in a recent review [12].

II. Methods

A. Computer Simulations of a Single Node of Ranvier

A model of a space-clamped patch of mammalian neural membrane was used to study the effects of subthreshold transmembrane polarization on neuronal excitability. The membrane patch was modeled based on voltage clamp studies of the nodal membrane of rabbit peripheral myelinated nerve fibers [4], [28], and included a nonlinear sodium conductance, a linear leakage conductance, and a membrane capacitance [Fig. 1(A)]. The first order differential equation describing the transmembrane potential [19] was solved using a second-order predictor corrector algorithm [9] implemented in PASCAL. A 2-ms simulation that computed and displayed transmembrane potential, transmembrane currents, and the values of the ion channel gating parameters took less than 3 s to run on a Macintosh Quadra 950. The effects of subthreshold membrane depolarization on excitability were studied by determining the threshold amplitude for excitation with different combinations of depolarizing prepulse (DPP) amplitude, DPP duration, interpulse delay, and stimulus duration.

B. Computer Simulations of Nerve Fiber Recruitment

A computer model of a mammalian myelinated nerve fiber was used to determine the effects of subthreshold DPP's on the relationship between the threshold current and the distance between the electrode and the nerve fiber. Nerve fibers were modeled using a 21-compartment cable model [Fig. 1(B)] with the nodes of Ranvier described by mammalian nonlinear membrane kinetics [4], [28] and the myelin assumed to be a perfect insulator [18]. All model parameters and assumptions were the same as those of Warman *et al.* [36]. The first order nonlinear differential equation describing the transmembrane voltage at each node was solved using the fourth-order Runge-Kutta method with doubling and halving of the time step [9] implemented in FORTRAN [28].

The model nerve fiber was positioned at different distances (0.25–1.5 mm) from a point current source directly above the middle compartment of the cable in a homogeneous, isotropic medium ($\rho = 55$ Ω-cm). An iterative method was used to determine threshold current (±1%) to generate propagating action potentials in 10-μm and 20-μm diameter nerve fibers with rectangular constant current pulses. A simulation run to determine the threshold current for one fiber configuration took approximately 2 min. on a Gateway 486/25. Criteria to recognize a propagating action potential were transmembrane voltage that exceeded 0 mV and a rate of change in transmembrane voltage that exceeded 60 mV/ms at a node five internodal lengths from the central node of the cable. It was important to consider propagating action potentials, as opposed to action potentials generate at the node directly under the electrode. Large stimulus currents created block of propagation by anodal surround (see Section III and [20]). The threshold amplitude for excitation with the stimulus pulse was determined as a function of the electrode to fiber distance for different combinations of prepulse amplitude, prepulse duration, and stimulus duration.

C. Experimental Measurements of Nerve Fiber Recruitment

Experiments were conducted in an animal model to determine the effects of subthreshold DPP's on the recruitment properties of direct nerve stimulation. All animal care and experimental procedures were according to National Institutes of Health (NIH) guidelines and were approved by the Institutional Animal Care and Use Committee of Case Western Reserve University. Silicone rubber spiral nerve cuff electrodes, containing 12 individually addressable platinum electrode contacts [35], were implanted on the right sciatic nerve of adult cats. The torques generated at the ankle joint by selective stimulation of the sciatic nerve were recorded. In this report, data are included from three acute experiments and five chronic experiments.

In acute experiments, animals were initially anesthetized with ketamine hydrochloride (35 mg/kg, I.M.), and atropine sulfate (0.05 mg/kg, I.M.) was administered to reduce salivation. Animals were intubated, a catheter was inserted in the cephalic vein, and a surgical level of anesthesia was maintained throughout the experiment with sodium pentobarbital (5–10 mg bolus injections, I.V.). For measurements with chronically implanted nerve cuff electrodes, animals were initially anesthetized with xylazine (Rompun, 2.0 mg/kg, SQ), masked with 3.0% gaseous Halothane in O_2, intubated, and

maintained at a surgical level of anesthesia with 1.5–2.0% gaseous Halothane in O_2. During both acute and chronic measurements, saline was administered (10 cc/kg/hour, IV) during the testing interval, body temperature was maintained with a heating pad, and heart rate and respiratory rate were continuously monitored.

Animals were mounted in a stereotaxic apparatus to measure the three-dimensional isometric torque generated at the ankle joint by stimulation of the sciatic nerve [11]. Twitch contractions in the ankle musculature were generated using controlled current rectangular pulses applied at 0.5 Hz. Monopolar electrode configurations with one contact in the cuff acting as the cathode and a 1.5 in. 22-gauge subcutaneous needle acting as the anode, and longitudinal tripolar electrode configurations with a dot cathode between two dot anodes within the cuff were used [35]. The interpolar spacing was 5 mm in the acute implants and 3 mm in the chronic implants. Two independent, isolated stimulator output stages were used to generate the prepulse and the stimulus pulse. The amplitude and duration of the prepulse were selected to be subthreshold, and the amplitude of the stimulus was stepped between threshold and maximum to generate recruitment curves of torque as a function of stimulus current amplitude using different depolarizing prepulses. An interleaved stimulus paradigm, where stimuli with and without the prepulse were applied alternately, was employed to avoid any time dependent changes (e.g., fatigue) that might affect the data. Stimulus amplitude was set manually with calibrated potentiometers while stimulus pulsewidth was controlled by the computer. The applied current waveform was monitored on a storage oscilloscope by differentially measuring the voltage generated in a 100-Ω resistor in series with the electrodes.

Stimulus control and response sampling were done using a multiple function input output board (NB-MIO-16H, National Instruments) in a Macintosh Quadra 950 and were controlled using software written in LabView (National Instruments). The torque signals were low pass filtered at 100 Hz and sampled at 200 Hz with a 12-b analog-to-digital converter. Five to ten twitch responses were collected at each stimulus amplitude and were averaged. The peak of the average torque twitch waveform was used as the measure of activation at each stimulus amplitude [11].

III. Results

A. *Effects of Subthreshold Depolarization on Neuronal Excitability*

Space Clamped Node of Ranvier: The effect of subthreshold membrane depolarization on the threshold current amplitude for a subsequent stimulus was studied using a model of a patch of mammalian neuronal membrane. Subthreshold DPP's decreased neuronal excitability and thus increased threshold for generation of an action potential by subsequent stimuli.

The transmembrane voltage response of a membrane patch to the two-pulse paradigm is shown in Fig. 2. The amplitude of the prepulse in this example (1268 $\mu A/cm^2$) was equal to 90% of the excitation threshold for a 500 μs duration pulse. As the time between the onset of the subthreshold DPP and the onset of the stimulus was increased (from A to C), the threshold for activation increased. The stimulus (100 μs, 1750 $\mu A/cm^2$) was sufficient to generate an action potential when applied without the DPP [Fig. 2(A)]. When the same stimulus was applied 200 μs after the onset of the DPP, it was also supra-threshold [Fig. 2(B)]. When the stimulus was applied 400 μs after the onset of the DPP it did not generate an action potential [Fig. 2(C)]. At this point the DPP had elevated threshold beyond the amplitude of the stimulus pulse. If the same stimulus was applied 500 μs after the cessation of the DPP, it again generated an action potential [Fig. 2(D)]. Thus, subthreshold depolarization caused a transient decrease in neuronal excitability and generated a transient increase in the threshold for stimulation.

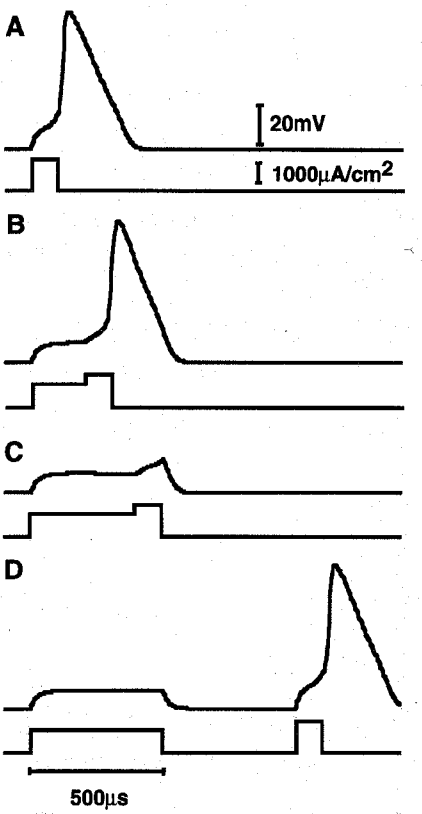

Fig. 2. Transmembrane potential responses of a space-clamped patch of nodal membrane to the two-pulse paradigm. The applied current, shown below each trace, consisted of a 100-μs stimulus pulse applied after subthreshold depolarization for (A) 0 μs, (B) 200 μs (C), 400 μs, or (D) after a 500-μs prepulse followed by a 500-μs delay. The amplitude of the prepulse was equal to 90% of threshold for a 500-μs duration stimulus (1268 $\mu A/cm^2$). The stimulus amplitude (1750 $\mu A/cm^2$) was the same for all traces.

The effect of subthreshold membrane depolarization on excitability varied with the duration and amplitude of the DPP, the delay between the DPP and the stimulus, as well as the duration of the stimulus (Fig. 3). Short duration DPP's decreased, rather than increased, threshold for stimuli of all durations that were tested. Longer duration DPP's increased threshold, and the magnitude of the increase varied with the duration of the stimulus pulse. Long duration DPP's coupled with long duration stimuli generated the maximal increases in threshold [Fig. 3(A)]. The increases in threshold generated by DPP's increased progressively as the amplitude of the DPP

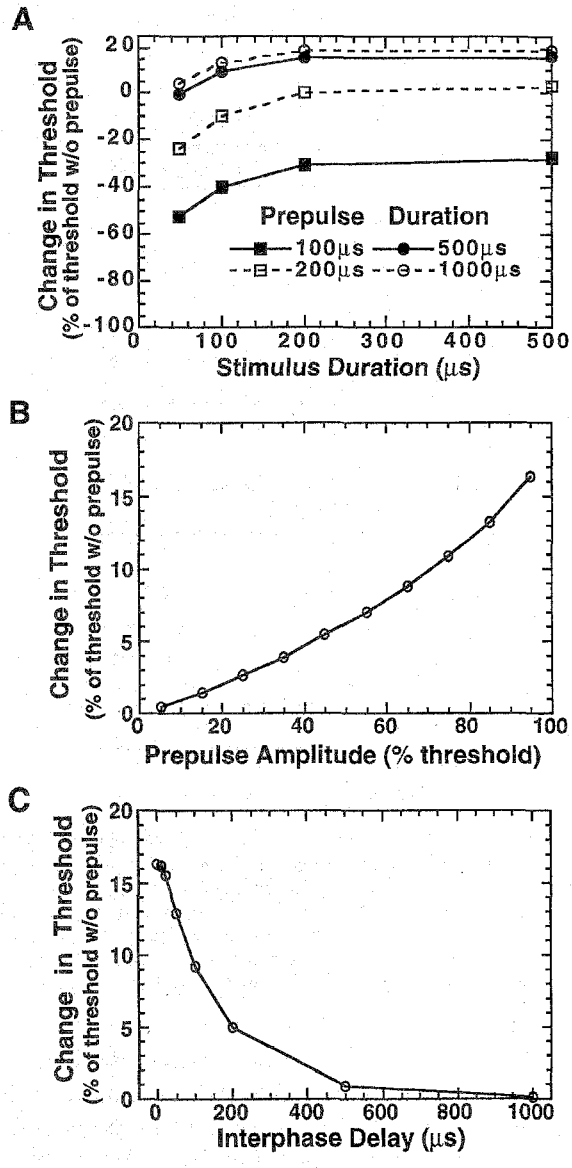

Fig. 3. Effect of prepulse and stimulus pulse parameters on the increase in threshold generated by the depolarizing prepulse: (A) Change in threshold, expressed as a percentage of the threshold without any prepulse, as a function of the stimulus pulsewidth for different duration depolarizing prepulses. The amplitude of the prepulse in each case was equal to 95% of the excitation threshold at that duration. (B) Change in threshold for excitation with a 500-μs stimulus pulse generated by a 500-μs depolarizing prepulse as a function of the amplitude of the prepulse. (C) Change in threshold generated by a 500-μs depolarizing prepulse with amplitude equal to 95% of threshold as a function of the delay between the end of the prepulse and the onset of a 500-μs stimulus pulse.

was increased from 5% of the excitation threshold to 95% of the excitation threshold [Fig. 3(B)]. The effects of DPP's decayed progressively as the interpulse delay between the prepulse and the stimulus was increased from 0 to 1000 μs [Fig. 3(C)]. Thresholds returned to those measured without any prepulse 500 μs after cessation of the prepulse. Thus, maximal decreases in excitability were generated for long DPP's with just subthreshold amplitudes followed at zero delay by stimulus durations of 100 μs or longer.

Cat Sciatic Nerve Fibers: Thresholds were measured experimentally for different combinations of DPP amplitude and duration and were compared to thresholds measured without any prepulse. In these experiments, threshold was defined as the current amplitude required to generate 2 N-cm of plantarflexion or dorsiflexion torque at the ankle joint. Long duration DPP's decreased neural excitability, thus increasing threshold for subsequent stimulation. The magnitude of the increase in threshold varied with the duration of the DPP. The increase in threshold generated by 500-μs DPP's, with amplitudes equal to 90–95% of the excitation threshold, ranged from 8–340% of the threshold without any prepulse (77 $\pm$ 117%, mean $\pm$ S.D., $n = 17$). Increases in threshold generated by 1000-μs DPP's, with amplitude equal to 90–95% of the excitation threshold, ranged from 25–78% of the threshold without any prepulse (54 $\pm$ 22%, $n = 7$). Longer duration DPP's generated larger increases in threshold for subsequent stimulation [Fig. 4(A)]. The magnitude of the increases in threshold also varied with the relative amplitude of the prepulse. Larger amplitude prepulses generated larger increases in threshold [Fig. 4(B)]. Thus, subthreshold depolarizing prepulses increased the threshold for activation of cat sciatic nerve motor fibers. As predicted by the modeling results (Fig. 3), the magnitude of threshold elevation varied with the prepulse parameters and the maximum elevations in threshold were obtained for long duration DPP's with an amplitude just below threshold.

B. Mechanism for Increases in Threshold

The values of the sodium channel gating parameters [16], $\mathbf{m}$ and $\mathbf{h}$, were tracked (Fig. 5) during the application of DPP's to illustrate the mechanism for the decreases in neuronal excitability (see [19] for a review of the Hodgkin Huxley description of neuronal excitability). The transmembrane potential and the values of the gating parameters during a subthreshold DPP followed by the same amplitude stimulus pulse either 100 μs [Fig. 5(A)] or 400 μs [Fig. 5(B)] after the onset of the stimulus pulse are shown in Fig. 5. The amplitude of the prepulse (1339 μA/cm^2) was equal to 95% of the excitation threshold of a 500-μs pulse. During the prepulse, the value of $\mathbf{h}$ was decreased at a constant rate, while the value of $\mathbf{m}$ increased rapidly to a plateau value slightly above the rest value.

Short duration DPP's caused an increase in excitability [Fig. 3(A)] as a result of the long time constant of the sodium inactivation gate. During a short (100 μs) DPP [Fig. 5(A)], the rapidly changing activation parameter, $\mathbf{m}$, increases ($\mathbf{m}$ increased by 1227% and $\mathbf{m}^2$ increased by 17 515%), but the inactivation parameter, $\mathbf{h}$, does not have time to decrease sufficiently to cause an elevation in threshold ($\mathbf{h}$ decreased by 20%). Thus, short duration depolarization lead to an increase, rather than a decrease, in excitability.

Long duration DPP's caused a decrease in excitability [Fig. 3(B)] by inactivation of the sodium channels. For long duration membrane depolarizations (400 μs), the value of $\mathbf{h}$ decreased (-58%), and the value of $\mathbf{m}$ decreased 15% relative to its peak value at 225 μs into the prepulse [Fig. 5(B)]. The result was a net decrease in neuronal excitability and an increase in threshold for subsequent stimuli.

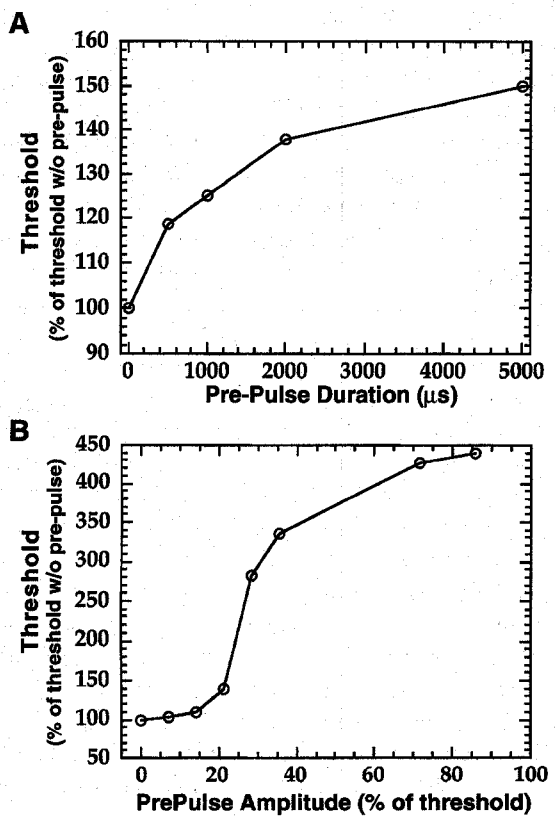

Fig. 4. Experimental measurements of the effect of prepulse parameters on threshold for excitation of cat sciatic nerve motor fibers: (A) threshold for a 500-μs stimulus pulse, expressed as a percentage of threshold measured without any prepulse, as a function of the duration of a depolarizing prepulse with amplitude equal to 95% of the excitation threshold at each prepulse duration and (B) threshold for a 500-μs stimulus pulse, expressed as a percentage of threshold measured without any prepulse, as a function of the amplitude of a 500-μs depolarizing prepulse.

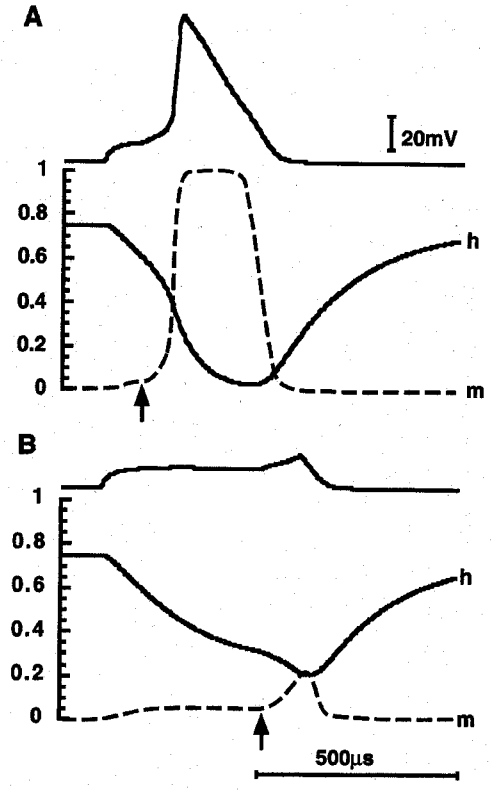

Fig. 5. Transmembrane potential $\mathbf{V_m}$ and the values of the sodium channel gating parameters **h** and **m** as a function of time generated by a subthreshold depolarizing prepulse followed by a 100-μs stimulus pulse at (A) 100 μs and (B) 400 μs after the onset of the prepulse. The arrow in each case illustrates the onset time of the stimulus pulse.

C. Effect of Depolarizing Prepulses on Neuronal Recruitment

Inversion of the Current-Distance Relationship: Cable models of 10-μm and 20-μm mammalian myelinated nerve fibers were used to study the effect of DPP's on the relationship between the threshold current and the distance between the electrode and the nerve fiber. With single 500-μs rectangular stimuli, the threshold current increased as the square of the distance between the electrode and the nerve fibers [Fig. 7(A)]. Furthermore, stimulation of smaller diameter nerve fibers (10 μm) required larger stimulus amplitudes than stimulation of larger diameter nerve fibers (20 μm).

Application of a subthreshold DPP before the stimulus elevated threshold for fibers close to the electrode. The increase in threshold was sufficient to allow stimulation of fibers lying more distant from the electrode at lower currents than required to stimulate fibers close to the electrode. The transmembrane potential at three nodes of two 20-μm model nerve fibers positioned 0.25 mm and 0.5 mm from the electrode is shown in Fig. 6. The applied current waveform was a 500-μs DPP with an amplitude (124 μA) equal to 90% of the threshold for the fiber at 0.25 mm followed by a 500-μs stimulus pulse. The DPP generated a subthreshold depolarization in both fibers, but the magnitude of the depolarization was larger in the

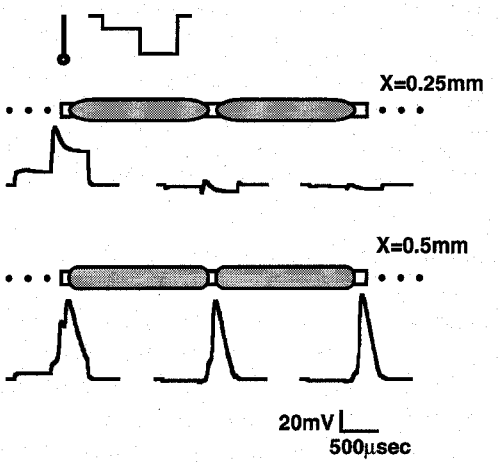

Fig. 6. Transmembrane voltage response of model myelinated nerve fibers positioned 0.25 mm and 0.5 mm from a point source stimulating electrode. The applied current was a 500-μs prepulse at 90% of the closer fiber's threshold followed by a 500-μs stimulus pulse that was supra-threshold for the fiber at 0.5 mm. Each trace is the transmembrane potential at that node as a function of time. The stimulus pulse generated a propagating action potential in the fiber at 0.5 mm, but not in the fiber at 0.25 mm.

closer fiber. The difference in depolarization caused a larger decrease in excitability of the fiber at 0.25 mm than the fiber at 0.5 mm. Thus, the subsequent stimulus pulse generated a propagating action potential in the fiber at 0.5 mm, but not in the fiber at 0.25 mm. The DPP waveform allowed stimulation of a fiber positioned further from the electrode at a lower

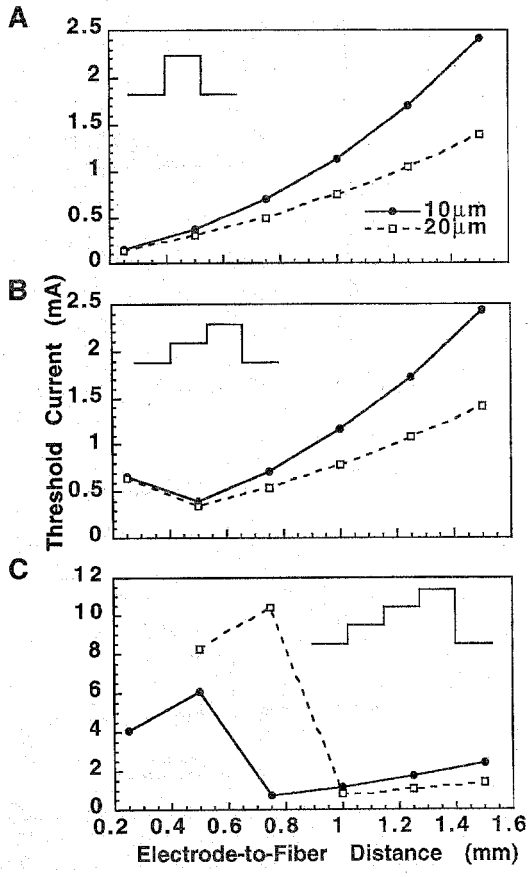

Fig. 7. Threshold current as a function of the distance between the point source electrode and 10-μm and 20-μm model nerve fibers: Current-distance relationship for (A) a monophasic 500-μs stimulus pulse, (B) a monophasic 500-μs stimulus pulse preceded by a 500-μs depolarizing prepulse with amplitude equal to 95% of the threshold for activation of a 20-μm fiber positioned 0.25 mm from the electrode, and (C) a monophasic 500-μs stimulus pulse preceded by a double 500-μs depolarizing prepulse. The amplitude of the first phase was equal to 95% of the threshold for activation of a 20-μm fiber positioned 0.25 mm from the electrode, and the amplitude of the second phase was equal to 95% of the threshold for activation of a 20-μm fiber positioned 0.5 mm from the electrode after the first step of the prepulse.

current amplitude than required to excite the fiber closer to the electrode.

The current-distance relationship for 10-μm and 20-μm nerve fibers after a 500-μs depolarizing prepulse with an amplitude (131 μA) equal to 95% of the excitation threshold for the 20-μm fiber at 0.25 mm is shown in Fig. 7(B). The DPP inverted the slope of the current-distance curve in the proximity of the electrode. The 20-μm fibers 0.5 mm and 0.75 mm from the electrode, and the 10-μm fibers 0.5 mm from the electrode, were stimulated at lower current amplitudes than required to stimulate the fibers 0.25 mm from the electrode. DPP's thus allowed selective stimulation of fibers lying more distant from the electrode at lower current amplitudes than required to excite fibers close to the electrode.

A stepped prepulse waveform was used to inactivate further fibers lying close to the electrode, and stimulate selectively even more distant nerve fibers [Fig. 7(C)]. The first prepulse (500 μs, 131 μA) elevated threshold for the closest fibers as seen above. A second DPP with an amplitude (500 μs, 333 μA) equal to 95% of the threshold for the most excitable fiber after the first prepulse (i.e., the 20-μm fiber 0.5 mm from the electrode) was then applied, followed at zero delay by a 500-μs stimulus pulse. The second step of the prepulse further elevated threshold for fibers close to the electrode, and inverted the current-distance curve over a larger distance than did the single DPP. The 10-μm fibers between 0.75 mm and 1.5 mm, and the 20-μm fibers between 1.0 mm and 1.5 mm, were stimulated at lower currents than fibers closer to the electrode. Stepped prepulse waveforms caused inversion of the current-distance curve over a larger region, and thus allowed selective activation of fibers even more distant from the electrode.

The transmembrane potential at individual nodes of the cable was monitored to follow action potential propagation. Using the stepped prepulse waveform [Fig. 7(C)], the threshold of the 20-μm fiber at 0.25 mm was elevated by more than seven times its value at rest. This large pulse amplitude generated strong hyperpolarization of the adjacent nodes that blocked action potential propagation [20]. Thus, following the stepped prepulse this fiber could not be activated at any stimulus amplitude. Also, in two cases, the site of initiation of the action potential shifted from the central node of the cable to the nodes that flanked the central node (10 μm fiber 0.5 mm from the electrode and 20 μm fiber 0.75 mm from the electrode). In these cases, the central node was inactivated to a degree that threshold was lower for excitation of the flanking nodes.

The stepped prepulse also allowed stimulation of small nerve fibers at lower stimulus amplitudes than large nerve fibers (i.e., natural recruitment order) at 0.75 mm from the electrode [Fig. 7(C)]. This was not unexpected since extracellular electric fields, whether stimulating or inactivating, affect large nerve fibers to a greater degree than small nerve fibers [6]. The DPP created a larger subthreshold depolarization in the large fibers and a greater degree of inactivation of the sodium conductance. There was a differential increase in threshold in the 20-μm fibers relative to the 10-μm fibers, and the 10-μm fibers were stimulated at a lower current amplitude than the 20-μm fibers.

Experimental Example: Using conventional rectangular stimuli, multiple contact nerve cuff electrodes generate selective activation of the fascicles closest to the active contact, followed by spillover of activation to fascicles further from the contact [14], [28], [35]. An example of this is shown by the results labeled "no prepulse" in Fig. 8. The active electrode (monopolar electrode configuration, 500-μs monophasic stimulus pulse) first generated plantarflexion torques as indicated by the positive deflection in the recruitment curve and the positive going twitch waveforms [11]. As the stimulus amplitude was further increased, the stimulus spread to excite the innervation of the muscles producing dorsiflexion at the ankle joint (i.e., the common peroneal fascicle of the sciatic nerve). This was seen as a decrease in the net torque at the joint and a negative deflection in the torque twitch waveform at 65 μA.

The model results demonstrating inversion of the current-distance relationship (Fig. 7) suggested that DPP's could be used to stimulate a fascicle lying further from an electrode without activating fibers close to an electrode. An example

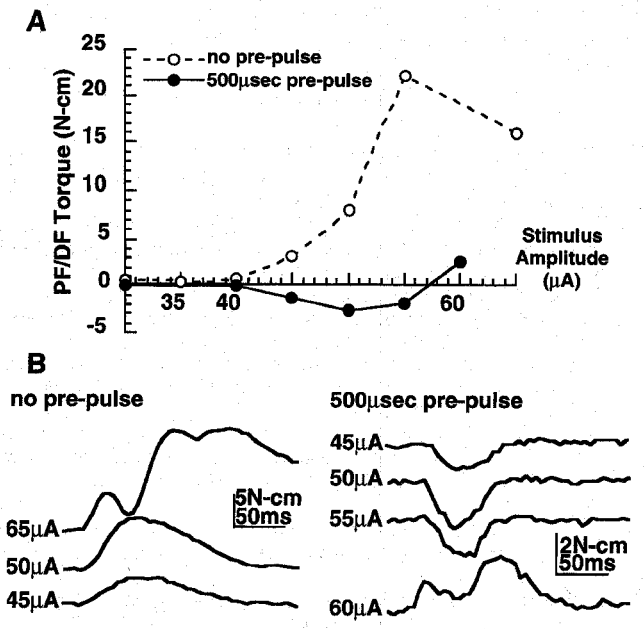

Fig. 8. Experimental measurement of the effect of a 500-μs depolarizing prepulse on the recruitment of cat sciatic nerve fascicles: (A) recruitment curve of the peak plantarflexion/dorsiflexion (PF/DF) ankle joint torque as a function of stimulus current amplitude of a 500-μs stimulus pulse or a 500-μs prepulse followed by a 500-μs stimulus pulse and (B) traces of the ensemble average of ten torque twitches generated by the indicated stimulus amplitude, either with or without a 500-μs prepulse. With a 500-μs stimulus pulse, plantarflexion torque was generated first as shown by the positive deflection of the recruitment curves and the positive going twitches. However, when the stimulus was preceded by a 500-μs prepulse, dorsiflexion torque was generated first as shown by the negative deflection in the recruitment curves and the negative going twitches.

of selective activation of the second recruited fascicle using a DPP is shown in Fig. 8. Using the same monopolar electrode contact, the stimulus pulse (500-μs monophasic) was preceded by a 500-μs DPP with amplitude (40 μA) equal to 90% of the excitation threshold. There was no delay between the cessation of the DPP and the onset of the stimulus pulse. When the DPP preceded the stimulus, dorsiflexion torques were generated at smaller current amplitudes than were plantarflexion torques. This was seen as a negative deflection in the recruitment curve and the negative going twitch waveforms. As the amplitude of the stimulus following the prepulse was increased, excitation spread to excite the innervation of the plantarflexor muscles. Thus, the pattern of torques generated using the DPP (dorsiflexion followed by spillover to plantarflexion) was the inverse of the pattern of torques generated using conventional rectangular stimuli (plantarflexion followed by spillover to dorsiflexion). These data demonstrate that depolarizing prepulses allowed stimulation of the second recruited fascicle before stimulation of the first recruited fascicle and provide experimental evidence indicating inversion of the current-distance relationship using subthreshold DPP's.

IV. Discussion

The results of this study demonstrate that the nonlinear conductances of neural membrane can be controlled to alter neuronal recruitment by electrical stimulation. Selective inactivation of fibers close to an electrode by subthreshold depolarizing prepulses elevated their threshold for subsequent stimulation, and enabled inversion of the current-distance relationship. Subthreshold depolarization decreased neuronal excitability by inactivation of the voltage dependent sodium channels. The state of inactivation produced by subthreshold membrane depolarization is analogous to the refractory period present after generation of an action potential.

Computer simulations and experimental measurements on cat sciatic nerve fibers indicated that maximal decreases in excitability were generated by long duration DPP's with just subthreshold amplitudes followed at zero delay by stimulus durations of at least 100 μs. The prepulse waveform, because of its long duration, requires more charge for excitation than conventional rectangular waveforms. For example, a 500-μs prepulse coupled with a 500-μs stimulus pulse would require 0.22-μC/phase (27 μC/cm^2), while a rectangular 100-μs stimulus pulse would require only 0.050 μC/phase (6.4 μC/cm^2). These calculations are based on an electrode contact diameter of 1mm and experimental measurements with a cuff electrode of the strength-duration characteristics of cat sciatic nerve fibers that yielded a rheobase current of 211 ± 75 μA (mean $\pm$ s.d., range = 94–353 μA, $n = 12$) and a chronaxie of 184 ± 84 μs (range = 67–342 μs). Although higher than conventional stimuli, the charge requirements of the prepulse waveform are smaller than the estimated reversible charge injection limits of platinum [21], and therefore should not limit the applicability of this technique.

The nerve fiber model predicted that selective inactivation would invert the current-distance relationship close to the electrode and allow fibers that were further from the electrode to be stimulated at currents smaller than required to stimulate fibers close to the electrode. The electric field model used to make these predictions was a homogeneous isotropic infinite medium rather than the inhomogeneous, anisotropic nerve trunk present in the biological system. Previous modeling studies have predicted that in an anisotropic cylinder the current-distance curve is sigmoidal [1] rather than parabolic as predicted by the isotropic model. However, experimental measurements of current-distance curves in anisotropic central nervous system structures indicate that the current-distance curve has a parabolic shape [2], [7], [22], [37]. The connective tissue layers around the nerve trunk were not included in the model and may also affect the region of excitation within the nerve [3], [34]. The success of the model in predicting the effects of depolarizing prepulses demonstrated the utility of such a model in cases where control of membrane excitability, rather than shaping of the excitatory field, was used for selective activation of the nervous system.

The other assumption of the fiber model was that the nodes of Ranvier were positioned directly under the stimulating electrode, while in the biological system there will be a distribution of nodal positions relative to the electrode, as incorporated in previous models [33], [34]. This assumption led to the prediction that the largest fibers closest to the electrode would have the lowest threshold. However, if the electrode was displaced laterally by one half of the internodal length, the model predicted that fibers with nodes positioned

directly under the electrode, but more distant from the electrode, would have lower thresholds than fibers closer to the electrode with the nodes displaced from directly beneath the electrode. Furthermore, with an offset electrode small fibers would be recruited at lower current amplitudes than large nerve fibers [12]. Experimental measurements with a cuff electrode indicate that large nerve fibers are invariably recruited at lower current amplitudes than small nerve fibers [6], and that nerve fascicles close to the electrode are stimulated at lower currents than fascicles further from the electrode [14], [29], [35]. Also, the experimental results of this study (Fig. 8) indicate that the prepulse is effective at inactivating fibers close to the electrode before those more distant from the electrode, and demonstrate activation first of a fascicle that was recruited second using conventional rectangular stimuli.

Modeling results indicated that stepped DPP's allow selective stimulation of small nerve fibers at lower currents than required for stimulation of large nerve fibers. Previous investigators have experimentally documented this effect of membrane depolarization. Zimmerman [26], [39] used very long duration (hundreds of milliseconds to seconds) depolarizing pulses to achieve differential block of large diameter nerve fibers and stimulate selectively small diameter nerve fibers. Similarly, Fukushima *et al.* [8] used very slowly rising current ramps to block differentially small caliber nerve fibers by membrane depolarization. However, the charge injection requirements to achieve this effect with the reported waveforms were very large. Charge injection for chronic neural prosthetic applications is limited by the requirement that the electrode not be corroded and the underlying tissue not be damaged [21]. Furthermore, very long duration pulses will preclude repetitive activation at the 10–50-Hz frequencies required for motor prosthetic applications. Another method to achieve selective activation of small nerve fibers is arrest of conduction in large nerve fibers by anodal block [6]. However, the long-duration waveforms used to cause anodal block must have an amplitude several times larger than threshold. Therefore this method also requires large charge injection for efficacy. Model results indicate that the stepped prepulse waveforms described in this study allow selective activation of small fibers using less injected charge.

Manipulation of the nonlinear properties of the neuronal membrane is a novel technique to control neuronal excitability. It provides another method, along with variations in electrode geometry and use of field steering currents, to activate selectively individual components of a peripheral nerve trunk. Importantly, these techniques may be applied using a cuff electrode which is the least invasive of the nerve-based electrodes and has the longest clinical history.

ACKNOWLEDGMENT

The authors wish to thank N. Caris, J. Crossen, and D. Tyler for assistance during the animal experiments, H. Kayyali for fabrication and maintenance of the laboratory stimulator, and M. Miller for development of the data collection software. The software for the model of the space clamped membrane patch was written by D. G. Atzberger and Z. H. Munir. The software for the fiber model was obtained from D. H. Perkel and modified by J. D. Sweeney and E. N. Warman.

REFERENCES

[1] K. W. Altman and R. Plonsey, "Point source nerve bundle stimulation: Effects of fiber diameter and depth on simulated excitation," *IEEE Trans. Biomed. Eng.*, vol. 37, pp. 688–698, 1990.

[2] E. V. Bagshaw and M. H. Evans, "Measurement of current spread from microelectrodes when stimulating within the nervous system," *Exp. Brain Res.*, vol. 25, pp. 391–400, 1976.

[3] R. R. Chintalacharuvu, D. A. Ksienski, and J. T. Mortimer, "A numerical analysis of the electric field generated by a nerve cuff electrode," in *Proc. 13th Int. Conf. IEEE-EMBS*, 1993, vol. 13, pp. 912–913.

[4] S. Y. Chiu, J. M. Ritchie, R. B. Rogart, and D. Stagg, "A quantitative description of membrane current in rabbit myelinated nerve," *J. Physiol.*, vol. 292, pp. 149–166, 1979.

[5] G. M. Clark, R. Black, D. J. Dewhurst, I. C. Forster, J. F. Patrick, and Y. C. Tong, "A multiple-electrode hearing prosthesis for cochlear implantation in deaf patients," *Med. Prog. Technol.*, vol. 5, pp. 127–140, 1977.

[6] Z.-P. Fang and J. T. Mortimer, "Selective activation of small motor axons by quasitrapezoidal current pulses," *IEEE Trans. Biomed. Eng.*, vol. 38, pp. 168–174, 1991.

[7] K. A. Follett and M. D. Mann, "Effective stimulation distance for current from macroelectrodes," *Exp. Neurol.*, vol. 92, pp. 75–91, 1986.

[8] K. Fukushima, O. Yahara, and M. Kato, "Differential blocking of motor fibers by direct current," *Pflügers Arch.*, vol. 358, pp. 235–242, 1975.

[9] S. A. Glantz, *Mathematics for Biomedical Applications*. Berkeley, CA: Univ. of Calif. Press, 1979, pp. 310–321.

[10] P. H. Gorman and J. T. Mortimer, "Effect of stimulus parameters on recruitment with direct nerve stimulation," *IEEE Trans. Biomed. Eng.*, vol. BME-30, pp. 407–414, 1986.

[11] W. M. Grill and J. T. Mortimer, "Non-invasive measurement of the input-output properties of peripheral nerve stimulating electrodes," *J. Neurosci. Methods*, vol. 65, pp. 43–50, 1996.

[12] ——, "Stimulus waveforms for selective neural stimulation," *IEEE Eng. Med. Biol. Mag.*, vol. 14, pp. 375–385, 1995.

[13] ——, "Effect of stimulus pulse duration on selectivity of neural stimulation," *IEEE Trans. Biomed. Eng*, vol. 43, pp. 161–166, 1996.

[14] ——, "Quantification of recruitment properties of multiple contact cuff electrodes," *IEEE Trans. Rehab. Eng.*, vol. 4, pp. 49–62, 1996.

[15] ——, "Selective activation of distant nerve fibers," in *Proc. 15th Int. Conf. IEEE-EMBS*, 1993, vol. 15, pp. 1249–1250.

[16] A. L. Hodgkin and A. F. Huxley, "A quantitative description of membrane current and its application to conduction and excitation in nerve," *J. Physiol.*, vol. 117, pp. 500–544, 1952.

[17] G. E. Loeb, "Neural prosthetic interfaces with the nervous system," *Trends in Neurosci.*, vol. 12, pp. 195–201, 1989.

[18] D. R. McNeal, "Analysis of a model for excitation of myelinated nerve," *IEEE Trans. Biomed. Eng.*, vol. BME-23, pp. 329–337, 1976.

[19] J. T. Mortimer, "Electrical excitation of nerve," in *Neural Prostheses: Fundamental Studies*, W. F. Agnew and D. B. McCreery, Eds. Englewood Cliffs, NJ: Prentice-Hall, 1990, , pp. 67–84.

[20] J. B. Ranck Jr., "Which elements are excited in electrical stimulation of mammalian central nervous system: A review," *Brain Res.*, vol. 98, pp. 417–440, 1975.

[21] L. S. Robblee and T. L. Rose, "Electrochemical guidelines for selection of protocols and electrode materials for neural stimulation," in *Neural Prostheses: Fundamental Studies*, W. F. Agnew and D. B. McCreery, Eds. Englewood Cliffs, NJ: Prentice-Hall, 1990, pp. 25–66.

[22] W. J. Roberts and D. O. Smith, "Analysis of threshold currents during microstimulation of fibers in the spinal cord," *Acta Physiol. Scand.*, vol. 89, pp. 384–394, 1973.

[23] K. L. Rodenhiser and F. A. Spelman, "A method for determining the driving currents for focused stimulation in the cochlea," *IEEE Trans. Biomed. Eng.*, vol. 42, pp. 337–342, 1995.

[24] W. L. C. Rutten, H. J. van Wier, and J. H. M. Put, "Sensitivity and selectivity of intraneural stimulation using a silicon electrode array," *IEEE Trans. Biomed. Eng.*, vol. 38, pp. 192–198, 1991.

[25] B. L. Rydevik, N. Danielsen, L. B. Dahlin, and G. Lundborg, "Pathophysiology of peripheral nerve injury with special reference to electrode implantation," in *Neural Prostheses: Fundamental Studies*, W. F. Agnew and D. B. McCreery, Eds. Englewood Cliffs, NJ: Prentice-Hall, 1990, pp. 85–105.

[26] M. Sassen and M. Zimmermann, "Differential blocking of myelinated nerve fibers by transient depolarization," *Pflügers Arch.*, vol. 341, pp. 179–195, 1973.

[27] R. A. Schindler and M. M. Merzenich, Eds., *Cochlear Implants*. New York: Raven, 1985.
[28] J. D. Sweeney, D. Durand, and J. T. Mortimer, "Modeling of mammalian myelinated nerve for functional neuromuscular stimulation," in *Proc. 9th Int. Conf. IEEE-EMBS*, vol. 9, pp. 1577–1578, 1987.
[29] J. D. Sweeney, D. A. Ksienski, and J. T. Mortimer, "A nerve cuff technique for selective excitation of peripheral nerve trunk regions," *IEEE Trans. Biomed. Eng.*, vol. 37, pp. 706–715, 1990.
[30] H. Thoma, W. Girsch, J. Holle, and W. Mayr, "Technology and long-term application of an epineural electrode," *Trans. Amer. Soc. Artif. Int. Organs*, vol. 35, pp. 490–494, 1989.
[31] B. Townshend and R. L. White, "Reduction of electrical interaction in auditory prostheses," *IEEE Trans. Biomed. Eng.*, vol. BME-34, pp. 891–897, 1987.
[32] C. H. van den Honert and J. T. Mortimer, "The response of the myelinated nerve fiber to short duration biphasic stimulating currents," *Ann. Biomed. Eng.*, vol. 7, pp. 117–125, 1979.
[33] P. H. Veltink, J. A. van Alste, and H. B. K. Boom, "Influences of stimulation conditions on recruitment of myelinated nerve fibers: A model study," *IEEE Trans. Biomed. Eng.*, vol. 35, pp. 917–924, 1988.
[34] P. H. Veltink, B. K. Van Veen, J. J. Struijk, J. Holsheimer, and H. B. K. Boom, "A modeling study of nerve fascicle stimulation," *IEEE Trans. Biomed. Eng.*, vol. 36, pp. 683–691, 1989.
[35] C. Veraart, W. M. Grill, and J. T. Mortimer, "Selective control of muscle activation with a multipolar nerve cuff electrode," *IEEE Trans. Biomed. Eng.*, vol. 40, pp. 640–653, 1993.
[36] E. N. Warman, W. M. Grill, and D. Durand, "Modeling the effects of electric fields on nerve fibers: Determining excitation thresholds," *IEEE Trans. Biomed. Eng.*, vol. 39, pp. 1244–1254, 1992.
[37] J. Yeomans, P. Prior, and F. Bateman, "Current-distance relations of axons mediating circling elicited by midbrain stimulation," *Brain Res.*, vol. 372, pp. 95–106, 1986.
[38] K. Yoshida and K. Horch, "Selective stimulation of peripheral nerve fibers using dual intrafascicular electrodes," *IEEE Trans. Biomed. Eng.*, vol. 40, pp. 492–494, 1993.
[39] M. Zimmermann, "Selective activation of C-fibers.," *Pflügers Arch.*, vol. 301, pp. 329–333, 1968.

Warren M. Grill Jr. (S'88–M'95) was born in Plainfield, NJ, in 1967. He received the B.S. degree in biomedical engineering in 1989 from Boston University, Boston, MA. He earned the M.S. degree in 1992 and the Ph.D. degree in 1995, both in biomedical engineering, from Case Western Reserve University, Cleveland, OH. During the summer of 1995 he attended the Neural Systems and Behavior course at the Marine Biological Laboratory, Woods Hole, MA.

He is presently a Research Associate in the Department of Biomedical Engineering at Case Western Reserve University. His research interests include neural prostheses, the electrical properties of tissues and cells, computational neuroscience, and neural control.

While a graduate student, Dr. Grill received awards for conference papers from IEEE-EMBS and RESNA.

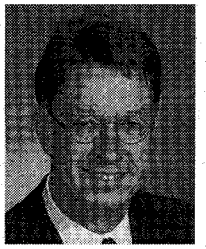

J. Thomas Mortimer, a native of Texas, he received the B.S.E.E. from Texas Technological College, Lubbock, the M.S. degree from Case Institute of Technology, Cleveland, OH, and the Ph.D. degree from Case Western Reserve University, Cleveland, OH.

He was Visiting Research Associate at Chalmers Tekniska Hogskola, Göteborg, Sweden from 1968 to 1969. He then joined the Department of Biomedical Engineering at Case Western Reserve University where he currently holds the title of Professor. He is also the Director of the Applied Neural Control Laboratory. In 1977–78 he was a Visiting Professor at the Institute für Biokybernetik und Biomedizinische Technik, Universität Karlsruhe, Karlsruhe, West Germany. In 1992 he was a Visiting Scholar at Tohoko University, Sendai, Japan. He is President of Axon Engineering, Inc., Willoughby, OH, a company providing electrodes and consulting services to parties interested in developing new products in the neural prosthesis area. His research interests concern electrically activating the nervous system. He holds nine patents in this area and has over 70 publications dealing with neural prostheses and related to pain suppression, motor prostheses for restoration of limb function and respiration, bladder and bowel assist, electrodes, and tissue damage and methods of selective activation.

In 1976, Dr. Mortimer was awarded the Humboldt-Preis by the Alexander von Humboldt Foundation, Federal Republic of Germany. He is a Founding Fellow of the American Institute for Medical and Biological Engineering. He was the recipent of the 1996 United Cerebral Palsy Research and Education Foundation's Isabelle and Leonard H. Goldenson Technology Award.